Front. Struct. Civ. Eng. 2022, 16(9): 1127–1140
https://doi.org/10.1007/s11709-022-0838-9

RESEARCH ARTICLE

Crack detection of the cantilever beam using new triple hybrid algorithms based on Particle Swarm Optimization

Amin GHANNADIASL*, Saeedeh GHAEMIFARD

Department of Civil Engineering, University of Mohaghegh Ardabili, Ardabil 56199-11367, Iran
**Corresponding author. E-mail: aghannadiasl@uma.ac.ir*

ABSTRACT The presence of cracks in a concrete structure reduces its performance and increases in the size of cracks result in the failure of the structure. Therefore, the accurate determination of crack characteristics, such as location and depth, is one of the key engineering issues for assessment of the reliability of structures. This paper deals with the inverse analysis of the crack detection problems using triple hybrid algorithms based on Particle Swarm Optimization (PSO); these hybrids are Particle Swarm Optimization-Genetic Algorithm-Firefly Algorithm (PSO-GA-FA), Particle Swarm Optimization-Grey Wolf Optimization-Firefly Algorithm (PSO-GWO-FA), and Particle Swarm Optimization-Genetic Algorithm-Grey Wolf Optimization (PSO-GA-GWO). A strong correlation exists between the changes in the natural frequency of a concrete beam and the crack parameters. Thus, the location and depth of a crack in a beam can be predicted by measuring its natural frequency. Hence, the measured natural frequency can be used as the input parameter of the algorithm. In this paper, this is applied to identify crack location and depth in a cantilever beam using the new hybrid algorithms. The results show that among the proposed triple hybrid algorithms, the PSO-GA-FA and PSO-GWO-FA algorithms are much more effective than PSO-GA-GWO algorithm for the crack detection.

KEYWORDS crack, cantilever beam, triple hybrid algorithms, Particle Swarm Optimization

1 Introduction

The existing crack within a structural component changes its local stiffness. So, vibration amplitudes and natural frequencies change due to the existence of such cracks. Therefore, it is feasible to determine crack location and depth by analysis of these changes. One of the methods of determining the crack location and depth is to utilize the mode shapes and the natural frequencies. An inverse method can be used for identification of structural damages. For this purpose, the optimization method is repeated to minimize or maximize the objective function so as to locate a crack. In this repeated operation, the unknown crack location can be located based on some parameters that can be updated using the optimization method to reach the best answer. Dimarogonas and Papadopoulos [1] and Qian et al. [2] prepared the stiffness matrix of the cracked beam and used intensity factors for investigation of the dynamic response characteristics such as the mode shapes and the natural frequencies. Nahvi and Jabbari [3] evaluated the failure intensity of cantilever cracked beams using the finite element method and experimental data. The lateral vibration of cracked Euler-Bernoulli beams was evaluated by Chondros et al. [4]. Also, Kim and Stubbs [5] investigated a feasible technique to calculate depths of cracks by utilizing modification in the natural frequencies. Orhan [6] studied the forced and free vibration analysis for recognizing cracks in a cantilever beam. Saavedra and Cuitino [7] explained the behavior of crack beams using the strain energy density function. Using a finite element manner, Zheng and Kessissoglou [8] investigated the natural frequencies and the mode shapes of a cracked beam. Rizos et al. [9] considered the flexural vibrations of a cantilever beam with surface crack. Sahoo and Maity [10] offered the hybrid Neuro-Genetic Algorithm (GA) to study crack parameters. Vakil-Baghmisheh et al. [11,12] investigated location and depth of cracks by utilizing the GA algorithm and hybrid techniques that compounded Nelder-Mead (NM) and Particle Swarm Optimization (PSO). Patil and Maiti [13] proposed the Transfer Matrix Technique for measurement

Article history: Received Jan 12, 2022; Accepted Feb 20, 2022

of locations of multiplex cracks using the measurement of natural frequencies. Rosales et al. [14] developed a technique to solve the inverse problem of crack location by compounding neural network methods with power series. Moezi et al. [15] precisely evaluated the crack location and depth in the beam using the Modified Cuckoo Optimization Algorithm. Nandwana and Maiti [16] explained crack discovery in a stepped beam with cracks, using models such as torsional spring. Lele and Maiti [17] developed a technique for short beams by utilizing measured frequencies to recognize the crack. Viola et al. [18] studied the cracked beam by obtaining the stable mass and stiffness matrices. Rezanezhad et al. [19] used the extended finite element method (XFEM), and modeled crack growth in a natural porous environment (like Fontainebleau sandstone).

Investigation of crack-location of 3D and 2D piezoelectric structures by utilizing XFEM methodology in the inverse and the direct problem are presented in Ref. [20,22–25]. Rabczuk and Belytschko [26] presented a novel technique for treating crack propagation by particle methods. Also, a geometrically non-linear three-dimensional cohesive crack was expressed using the extended element-free Galerkin method for reinforced concrete structures [27]. Ghasemi et al. [28,29] investigated the behavior of flexoelectric composites using the computational design method, location Isogeometric Analysis (IGA), and point-wise density mapping techniques. Also, Ghasemi et al. [30,31] studied probabilistic multi-constraints optimization of cooling channels in ceramic matrix composites (CMC) and a reinforcement distribution optimizer based on Non-uniform Rational B-spline (NURBS) as a methodology for decreasing interfacial stresses in sandwich beams. Talebi et al. [32] presented multiscale modeling of three-dimensional crack and dislocation propagation. Zhou et al. [33–35] presented a Phase-Field Model (PFM) for simulating complex crack patterns including crack propagation, branching, and coalescence in rock and poroelastic media using an implicit time integration scheme and the Newton–Raphson iteration in commercial finite element software COMSOL. In previous research, the applied techniques were extended for crack recognition in beams. Therefore, various methods and algorithms have been used in recent years to identify the presence of cracks in beam structures. Table 1 presents a short review of some researches and their applied techniques. In this paper, a procedure is applied to evaluate the locations and depths of cracks in cantilever beams, which improves the precision of crack detection. In this study, new hybrid algorithms are utilized for crack detection of cantilever beams. These triple hybrid algorithms combine GA, PSO, Grey Wolf Optimization (GWO), and Firefly Algorithm (FA). These algorithms are used to minimize the cost function to detect the locations and depths of cracks in cantilever beams. In other words, this paper uses Particle Swarm Optimization-Genetic Algorithm-Grey Wolf Optimization (PSO-GA-GWO), Particle Swarm Optimization-Genetic Algorithm-Firefly Algorithm (PSO-GA-FA), and Particle Swarm Optimization-Grey Wolf Optimization-Firefly Algorithm (PSO-GWO-FA) algorithms for evaluating tasks to obtain the best results. Finally, the results obtained from these triple algorithms are compared with other algorithms such as GA, GWO, FA, PSO, and Modified Particle Swarm Optimization (MPSO).

2 Modelling of the cracked beam

In this paper, the cantilever beam is considered as shown in Fig. 1. This beam has length "L", width "b", depth of the crack "a" at changeable location L_1, and thickness "h". The flexibility matrix is represented via stress intensity factors, and the existence of a transverse surface crack affects the dynamic efficiency of the construction. The relation between the stress intensity factors and the strain energy release rates at the crack segment has been presented by Jena and Parhi [36]. Also, by considering the reverse of the flexibility matrix [1], the local stiffness matrix can be obtained. The differential equations of the free vibration of an Euler-Bernoulli beam can be determined as:

$$EI\frac{\partial^4 W}{\partial X^4}+m\frac{\partial^2 W}{\partial t^2}=0, \tag{1}$$

$$\left(\frac{E}{\rho}\right)\frac{\partial^2 V}{\partial X^2}=\frac{\partial^2 V}{\partial t^2}. \tag{2}$$

Equation (1) applies to transverse vibration, and Eq. (2) applies to the longitudinal vibration; m is the unit mass of the length of the beam; W and V demonstrate the transverse and longitudinal movements; ρ is the density. The responses of the transverse vibration and the longitudinal vibration are determined according to the method applied in Ref. [37]. The cracked beam is separated into two segments of left and right ($x \in [0,L_1]$) and $x \in (L_1,L]$). Therefore, we have:

$$W_{\mathrm{R}}(x)=C_{\mathrm{R1}}\cosh\left(\frac{\lambda x}{L}\right)+C_{\mathrm{R2}}\sinh\left(\frac{\lambda x}{L}\right)+C_{\mathrm{R3}}\cos\left(\frac{\lambda x}{L}\right)+C_{\mathrm{R4}}\sin\left(\frac{\lambda x}{L}\right), \tag{3a}$$

$$W_{\mathrm{L}}(x)=C_{\mathrm{L1}}\cosh\left(\frac{\lambda x}{L}\right)+C_{\mathrm{L2}}\sinh\left(\frac{\lambda x}{L}\right)+C_{\mathrm{L3}}\cos\left(\frac{\lambda x}{L}\right)+C_{\mathrm{L4}}\sin\left(\frac{\lambda x}{L}\right), \tag{3b}$$

$$V_{\mathrm{R}}(x)=C_{\mathrm{R5}}\cos\left(\lambda\frac{x}{L}\right)+C_{\mathrm{R6}}\sin\left(\lambda\frac{x}{L}\right), \tag{4a}$$

Table 1 A summary review of recent developments in crack identification of beam structures

author	target	applied technique	results	constraint
Ghadimi and Kourehli [38]	using modified extreme learning machine	modified ELM	rapid convergency in estimating the crack	N/A
Ghadimi and Kourehli [39]	using extreme learning machine	ELM	fast approach in detection crack in spite of noisy data	considering uncracked elements as crack with low value of crack depth ratio
Prawin and Rama Mohan Rao [40]	using baseline free algorithm	Fourier power spectrum	good approach by using an enhanced spatial fourier power spectrum	N/A
Ghadimi and Kourehli [41]	using ELM and LSM for detect crack in beam structures under moving mass	ELM and least square support vector machine	reliable tool to accurately identify cracks in beam structures under moving mass	LS-SVM has better accuracy than ELM in detection of crack
Samir et al. [42]	using orthogonal decomposition method and cuckoo search algorithm in CFRP	orthogonal decomposition method and cuckoo search	POD-RBF-CS and POD-RBFGA have good function in prediction crack size and location	It does not stabilize when noise levels are higher than 6%.
Khatir et al. [43]	using PSO–FEM method	PSO	excellent estimation of the crack depth and location of cantilever beam and 2D frame	N/A
Wimarshana et al. [44]	using entropy method in detection of breathing cracks in a beam	entropy method	good function by using this method in detection breathing crack	failure to detect cracks with low excitation frequency with entropy method
Wei et al. [45]	using vibration data	improved PSO	detection of crack in beam, truss and plate by improved PSO	is effective only with measurement noise
Khatir et al. [46]	using teaching−learning-based optimization algorithm	teaching−learning optimization	high accuracy of TLBO in detection of crack	N/A
Zenzen et al. [47]	using frequency response function and bat	FRF method, BAT algorithms	high precision and computational time of BAT algorithm	increase of number of degrees of freedom leads to high computational costs
Wang et al. [48]	using bayesian inference and closed-form solution of vibration modes	Bayesian inference	higher precise in detection of crack location than detection of depth in beams with multiple cracks	failure to quantify identification of crack
Chinka et al. [49]	using mode shape curvatures and natural frequencies	frequency-mode shape	using frequency /mode shape based damage detection technique (FMBDD) method for easily achieving accurate results	N/A
Wu et al. [50]	using homotopy analysis algorithm	homotopy analysis algorithm	HDI, FPDI and MC methods all acheived good accuracy in detection of crack	N/A
Broumand [51]	using extended finite element concepts for multiple crack detection in 2D elastic continua	crack detection based on residual error (CDRE) and crack detection based on stiffness residual (CDSR) methods	CDRE method has higher accuracy in crack detection than CDSR method.	N/A
Zainud-Deen et al. [21]	detection angular crack and its location in a conductor system	hybrid finite difference frequency domain -PSO	crack location, width, and depth can be successfully reconstructed	N/A
Viola et al. [18]	development of the stiffness and the consistent mass matrices for a two-node cracked Timoshenko beam	finite element method	using modal test data for identifying cracks in structures	N/A

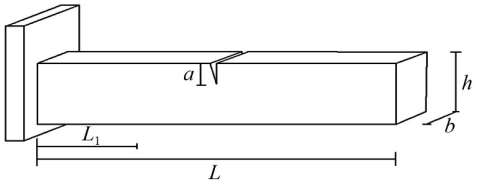

Fig. 1 The shape of the cantilever beam containing crack.

$$V_{\mathrm{L}}(x) = C_{\mathrm{L}5}\cos\left(\lambda\frac{x}{L}\right) + C_{\mathrm{L}6}\sin\left(\lambda\frac{x}{L}\right). \tag{4b}$$

The term λ (in Eqs. (3a), (3b), (4a), and (4b)) is dependent on the natural frequency of the beam, (i.e., $\lambda^4 = \rho A\omega^2/\mathrm{EI}$). Also, $C_{\mathrm{R},i}$ = 1:6, and $C_{\mathrm{L},i}$ = 1:6 are the unknown coefficients that can be defined using suitable boundary conditions and the continuity conditions at the cracked section. The relations can be expressed according to Ref. [37]. The equation of the system can be shown as $|\boldsymbol{B}| = 0$ that contains the local stiffness matrix [36]. This is a function of the non-dimensional crack depth, natural frequency (ω), and function of the relative locations of the crack (α). Matrix $\boldsymbol{B}$ is shown explicitly in Appendix.

3 Objective function formulation for locating a crack by utilizing optimization algorithms

As mentioned in the above sections, recognizing variations of the natural frequencies of the cracked beams for a special location and depth of crack is an easy process. Evaluating the unknown location and depth of cracks repeatedly by utilizing an optimization algorithm is the

purpose of the inverse technique, which leads to calculation of the real and the evaluated natural frequencies. The minimized objective function of the inverse problem can be considered as:

$$\mathrm{Min}f(l_c, d_c) = \sum_{i=1}^{m} \left[\varphi_i \left(f_i^{\mathrm{d}} - f_i^{\mathrm{s}}\right)\right]. \quad (5)$$

The optimization algorithm searches the location and depth of cracks in a manner in which the summation of variations among the evaluated and measured frequencies is minimized to zero. According to the restriction, it is assumed $0 < a < h$ and $0 < L1 < L$. In Eq. (5), "m" is the number of natural frequencies, "φ_i" is the ith weighting factor, "f_i^{d}" is the ith demanded natural frequency of a cracked beam, "f_i^{s}" refers to the ith natural frequency that is evaluated by the algorithm and utilized to estimate the objective function. In this paper, the first three natural frequencies of a cracked beam (FNF, SNF, and TNF) are used as inputs of the crack discovery problem to measure the objective function. Also, the weighting factors, φ_i's, are considered as $\frac{1}{I}$ [52,53]. PSO is an evolutionary optimization method offered by Kennedy and Eberhart [54]. PSO uses a society-dependent universal probe method in which every single particle behaves as particle of the flock to apportion data between them such as to obtain a universal optimum. GA is a heuristically probing algorithm based on natural selection. GA forms an intelligent expansion of a random probe within a determined search area to solve a problem. This algorithm uses a society of persons that are subject to mutability-compelling factors like mutation and crossover. Also, a compatibility function is utilized to appraise persons and reproductive achievement changes with compatibility. FA is based on the behavior of fireflies, a type of insect. Most fireflies produce rhythmical and partial sparkles [55,56]. GWO has been widely applied to many optimization problems due to its advantages over other swarm intelligence techniques. Moreover, the leadership, hierarchy, and quarrying craft of grey wolves in nature are displayed. Also, four kinds of grey wolves denoted as omega (ω), delta (δ), beta (β), and alpha (α) are offered to model the hierarchy [57].

3.1 Hybrid algorithms functions

This section explains the new hybridized algorithms involving PSO, GA, FA, and GWO algorithms. The proposed triple hybrid algorithms (PSO-GA-FA, PSO-GWO-FA, PSO-GA-GWO) have been extended without changing the basic operation of the PSO, FA, GA, and GWO algorithms. It is already known that the PSO algorithm achieves better results in almost all real-world problems; but existence of a solution is needed to reduce the possibility that the PSO algorithm will become trapped in a local minimum. In the proposed method, the GWO, FA, and GA algorithms are utilized to support the PSO algorithm to decrease the likelihood of falling into a local minimum.

3.1.1 Particle Swarm Optimization-Genetic Algorithm-Firefly Algorithm

The intention of combining three evolutionary algorithms PSO, GA, and FA to create the hybrid PSO-GA-FA is based on natural selection. GA that makes the 'offspring' seize the favored genetic structure from parents. In this hybrid algorithm, PSO obtains a good outcome for every individual, and these experiences aid FA to get a better survival chance in the symbiotic interplay. As the basic actions in the natural selection repeatedly do, it requires to run the GA, PSO, and FA algorithms consecutively to simulate these actions. Figure 2 presents the schematic view of the proposed PSO-GA-FA algorithm. As can be seen, this method consists of 3 main phases (PSO, GA, and FA), which are executed consecutively.

3.1.2 Particle Swarm Optimization-Genetic Algorithm-Grey Wolf Optimization

The theory of compounding GWO, PSO, and GA are considered for dominating problems of the algorithms mentioned above and getting the accurate response for recognition of a crack in a cantilever beam. PSO-GA-GWO together can provide better results than PSO, GWO, and GA individually. Firstly, determining the objective function, variables, and any parameter of the algorithm is essential. This method searches the optimum answer till the stopping criteria are found, or repetition ends location. When appraisal and repetition of PSO ends, GA begins acting by solving optimization problems involving people selection, crossover, and mutation. Thereafter, GWO starts its action. The sequence of actions of the suggested algorithm PSO-GA-GWO is shown in Fig. 3.

3.1.3 Particle Swarm Optimization-Grey Wolf Optimization-Firefly Algorithm

By embedding the GWO and FA operators in PSO, equilibrium among the discovery and extraction capability is amended better. First of all, the objective function, variables, and any algorithm parameter should be determined. This procedure searches the optimum values of objective function by updating the location and velocity of the results till the stopping criteria are found, or repetition ends. When assessment and repetition of the results ends in PSO, GWO begins to act and carry on to solve the optimization problem. Then, FA starts its action

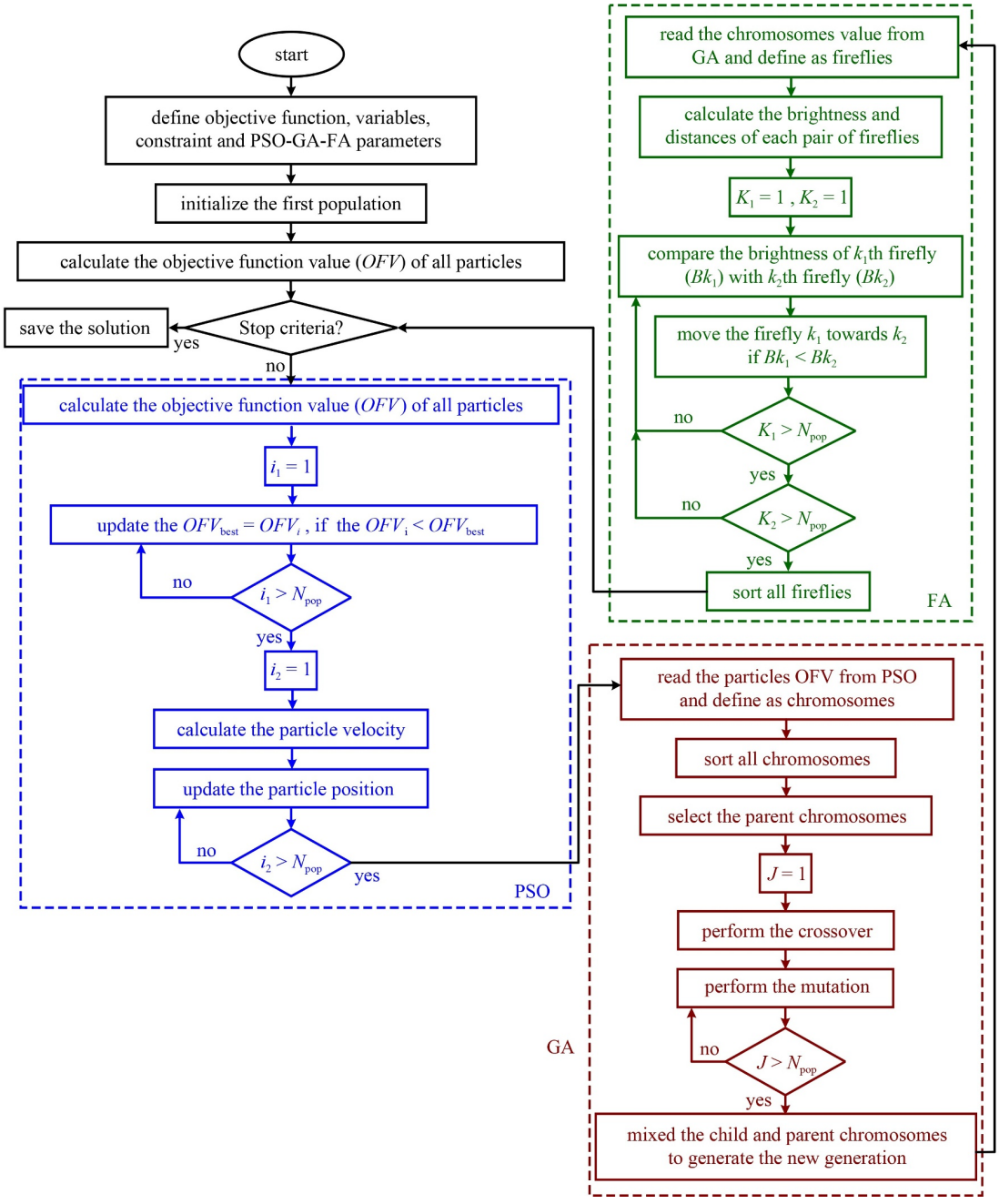

Fig. 2 PSO-GA-FA flowchart.

by assessing fireflies' brightness and updating them until the repetition ends. The process of optimizing with the PSO-GWO-FA algorithm is displayed in Fig. 4. Also, the pseudocode of the proposed algorithms is described in Pseudocode 1. On this pseudocode, first main subroutine runs and then first PSO subroutine runs and by attention to the algorithms, the following subroutine runs.

4 Discussion

The geometrical and mechanical properties of the considered beam are introduced in Table 2. The natural frequencies of the Euler-Bernoulli beam for various locations and depths of cracks are presented in Table 3. In this paper, the method applied in Ref. [58]. is used to determine the natural frequencies of a cracked Euler-Bernoulli beam. In this section, the technique of detecting cracks in the cantilever beam is presented by the proposed algorithms. It aims to detect location and depth of a crack by optimizing the objective function based on the natural frequencies of the beam. Thus, the results of the crack detection in the cracked beams are reported by the presented algorithms. In this paper, five algorithms

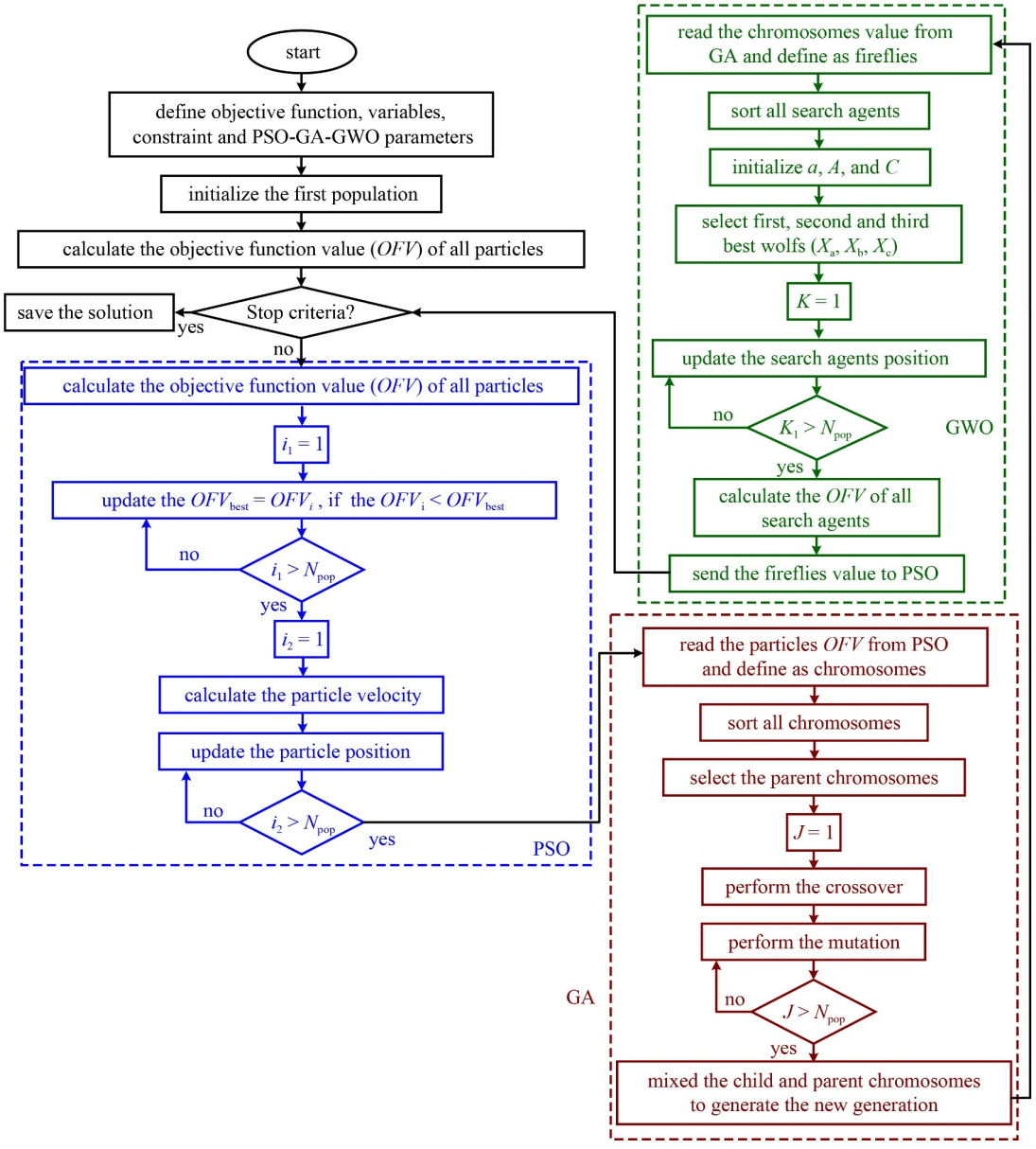

Fig. 3 PSO-GA-GWO flowchart.

(GA, GWO, FA, PSO, and MPSO) were compared.

Three sets of the control parameters are chosen for evaluating various strategies of the proposed algorithms, as explained in Table 4. In each set, the number of populations is different, so sets A, B, and C equal 10, 21, and 32, respectively. The control parameters of the PSO algorithm such as inertia weight parameter, W, Cognitive parameter, C_1, and Social parameter, C_2, have the same values in all sets and other parameters have different values. To compare the achieved results of the present study with the results of Jena and Parhi [36], the properties of the cantilever beam based on their data are considered. The proposed triple hybrid algorithms are investigated by comparison with the results of Jena and Parhi [36] for six cases. These comparisons are shown in Tables 5 and 6 for set A. Tables 7 and 8 show the results of PSO, GA, FA, and GWO algorithms in identification of crack location and depth for set A. To demonstrate the effectiveness of the proposed triple hybrid algorithms, a performance index is defined. This index reports the variance between evaluated and actual values of parameters. This performance index is defined as follows:

$$\%error = \left|\frac{D_2 - D_1}{D_2}\right| \times 100. \tag{6}$$

The index is applied to comparing the results from the proposed algorithms. Tables 5 and 6 suggest that the performance of the PSO-GA-FA algorithm is better than the PSO-GA-GWO algorithm and that is better than the PSO-GWO-FA algorithm. The results show that the

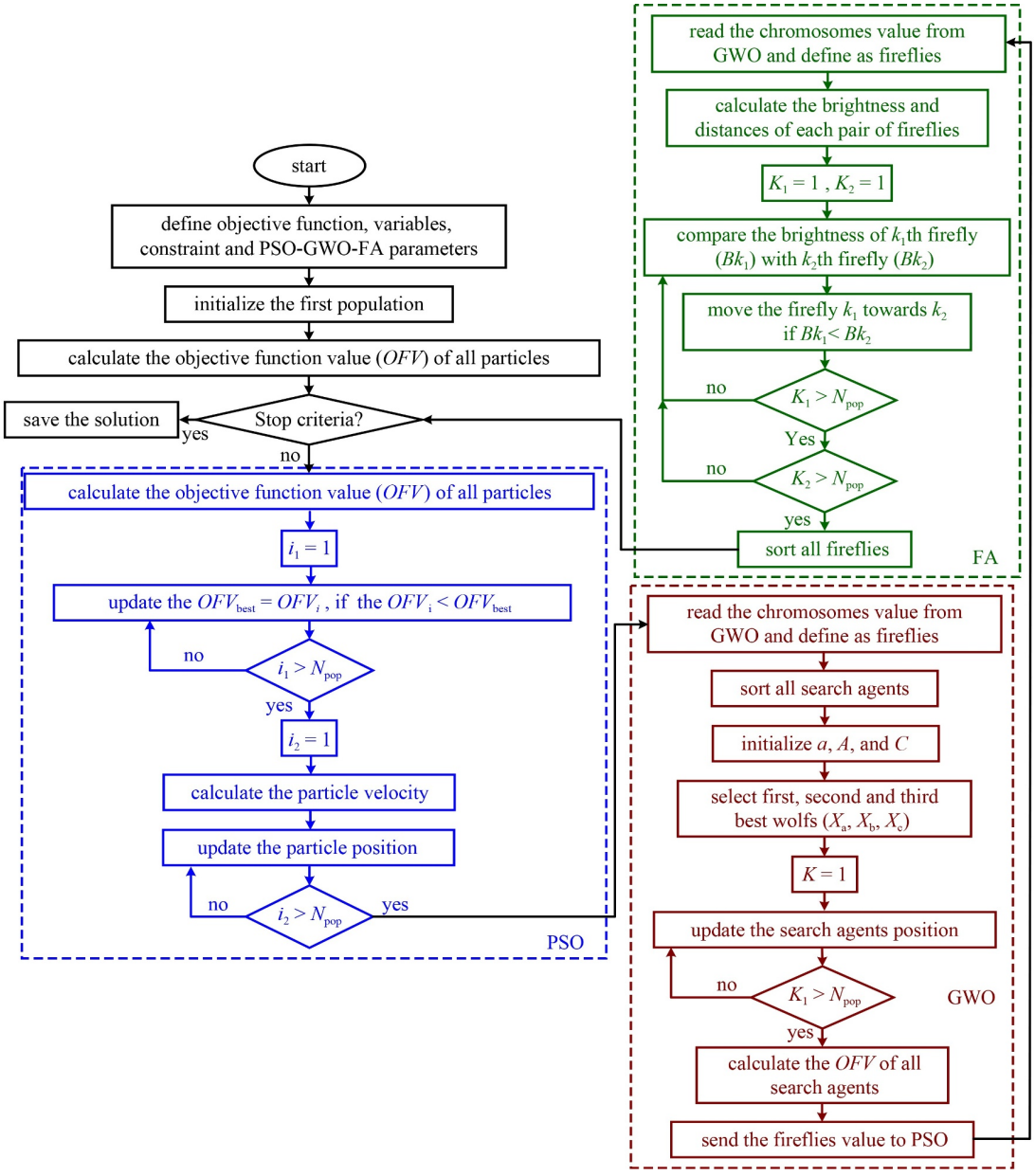

Fig. 4 PSO-GWO-FA flowchart.

Table 2 Material properties and geometry of the beam

parameter	value
height, h	6 mm
length, L	800 mm
Poisson's ratio, μ	0.33
density, ρ	2.8 g/cm^3
width, W	50 mm
Young's modulus, E	72.4 GPa

average calculation errors for crack location and depth equivalent, respectively, are 2.04×10^{-3}% and 2.79×10^{-1}% for the PSO-GA-FA algorithm while reaching 1.1×10^{-3}% and 2.62×10^{-1}% for the PSO-GA-GWO algorithm, 1.81×10^{-2}% and 1.54×10^{-1}% for the PSO-GWO-FA algorithm. Finally, based on findings in this study, the crack location and depth are more accurately determined by the proposed algorithms. Also, Tables 7 and 8 indicate that PSO performs better than GWO, and GWO is higher in convergence GA, with the performance indexes for crack location and depth equivalent to 2.73×10^{-4}% and 2.01×10^{-1}% for PSO while reaching 4.97×10^{-1}% and 9.73×10^{-1}% for GA, 3.24×10^{-1}% and 2.94×10^{-1}% for GWO, and 3.25×10^{-2}% and 2.0×10^{-1}% for FA.

Figure 5 displays the convergence of algorithms based on set A for the cracked beam model via the existence of crack case no. 6. Figure 5(a) clearly shows that FA has a higher convergence than others. On the other hand,

Fig. 5(b) illustrates that the PSO-GA-FA algorithm has the best convergence in comparison with the proposed algorithm in the identification of the location and depth of cracks.

Figure 6 shows the convergence characteristics of the proposed triple algorithms that have the most errors for crack detection. In Figs. 7−10, the convergences of the triple hybrid algorithms for the cracked beam model to find the crack location and depth for cases no. 2, 4, 8, and 10 are shown for all sets of control parameters. Also, the

Table 3 The natural frequencies for cracked beam cases

case no.	crack (mm)		natural frequencies (Hz)		
	Loc.	Dep.	FNF	SNF	TNF
1	no crack	no depth	7	45	140
2	200	1.2	7.699	48.260	135.108
3	200	1.8	7.693	48.258	135.024
4	200	2.4	7.678	48.254	134.826
5	400	1.2	7.700	48.248	135.131
6	400	1.8	7.698	48.202	135.131
7	400	2.4	7.694	48.096	135.131
8	600	1.2	7.700	48.256	135.095
9	600	1.8	7.700	48.240	134.964
10	600	2.4	7.700	48.204	134.657

Note: FNF, SNF, and TNF represent the 1st, 2nd, and 3rd natural frequencies, respectively.

Table 4 Variant collection of control parameters to solve the optimization problem of the cracked beam

optimization parameters	value		
	set A	set B	set C
population size	10	21	32
inertia weight parameter of PSO, W	0.5	0.5	0.5
cognitive parameter of PSO, C_1	2	2	2
social parameter of PSO, C_2	2	2	2
mutation	0.2	0.3	0.4
crossover	0.8	0.85	0.95
γ of FA	1	0.9	0.8
β_0 of FA	2	1.9	1.8
α of FA	0.2	0.1	0.3
maximum number of iterations (max_iter)	100	200	300

Table 5 Failure calculation of the location of crack obtained from PSO-GWO-FA, PSO-GA-FA, PSO-GA-GWO, and MPSO for set A

precise value (mm)		PSO-GWO-FA Loc. (*%error*)	PSO-GA-FA Loc. (*%error*)	PSO-GA-GWO Loc. (*%error*)	MPSO [36] Loc. (*%error*)
Loc.	Dep.				
200	1.2	200 (0)	200 (0)	199.999 (0.0005)	–
	1.8	200 (0)	199.999 (0.0005)	199.999 (0.0005)	200.16 (0.08)
	2.4	199.989 (0.0055)	200 (0)	200 (0)	199.88 (0.06)
400	1.2	399.999 (0.00025)	400 (0)	399.999 (0.00025)	–
	1.8	399.999 (0.00025)	399.999 (0.00025)	400 (0)	400.24 (0.06)
	2.4	400 (0)	399.955 (0.0112)	399.999 (0.00025)	399.80 (0.05)
600	1.2	600.505 (0.0841)	600 (0)	599.989 (0.0001)	–
	1.8	600.047 (0.0078)	600.038 (0.0063)	599.992 (0.0013)	599.76 (0.04)
	2.4	599.605 (0.065)	599.999 (0.00016)	600.042 (0.007)	600.18 (0.03)

Table 6 Failure calculation of the depth of crack obtained from PSO-GWO-FA, PSO-GA-FA, PSO-GA-GWO, and MPSO for set A

precise value (mm)		PSO-GWO-FA Dep. (*%error*)	PSO-GA-FA Dep. (*%error*)	PSO-GA-GWO Dep. (*%error*)	MPSO [36] Dep. (*%error*)
Loc.	Dep.				
200	1.2	1.2 (0)	1.19 (0.84)	1.2 (0)	–
	1.8	1.79 (0.555)	1.8 (0)	1.8 (0)	1.802 (0.11)
	2.4	2.4 (0)	2.39 (0.416)	2.39 (0.416)	2.398 (0.08)
400	1.2	1.2 (0)	1.19 (0.84)	1.2 (0)	–
	1.8	1.8 (0)	1.8 (0)	1.79 (0.555)	1.802 (0.11)
	2.4	2.39 (0.416)	2.4 (0)	2.4 (0)	2.4 (0)
600	1.2	1.2 (0)	1.2 (0)	1.19 (0.84)	–
	1.8	1.8 (0)	1.8 (0)	179 (0.555)	1.801 (0.05)
	2.4	2.39 (0.416)	2.39 (0.416)	2.4 (0)	2.4 (0)

Table 7 Failure calculation of the location and depth of crack obtained from PSO and GA algorithms for set A

precise value(mm)		PSO		GA	
Loc.	Dep.	Loc. (%error)	Dep. (%error)	Loc. (%error)	Dep. (%error)
200	1.2	199.999 (0.0005)	1.2 (0)	199.963 (0.0185)	1.2 (0)
	1.8	199.999 (0.0005)	1.8 (0)	204.186 (2.093)	1.77 (1.66)
	2.4	199.999 (0.0005)	2.39 (0.416)	201.996 (0.988)	2.38 (0.833)
400	1.2	399.999 (0.00025)	1.2 (0)	400.121 (0.030)	1.21 (0.84)
	1.8	400 (0)	1.79 (0.555)	400.255 (0.0637)	1.74 (3.333)
	2.4	399.999 (0.00025)	2.4 (0)	400.142 (0.0355)	2.39 (0.416)
600	1.2	599.999 (0.00016)	1.19 (0.84)	594.201 (0.966)	1.19 (0.84)
	1.8	600 (0)	1.8 (0)	600.027 (0.0045)	1.8 (0)
	2.4	600.002 (0.0003)	2.4 (0)	598.310 (0.2816)	2.38 (0.84)

Table 8 Failure calculation of the depth and the location of crack obtained from FA and GWO algorithms for set A

precise value (mm)		GWO		FA	
Loc.	Dep.	Loc. (%error)	Dep. (%error)	Loc. (%error)	Dep. (%error)
200	1.2	200.593 (0.296)	1.19 (0.84)	199.858 (0.071)	1.2 (0)
	1.8	200.299 (0.149)	1.79 (0.555)	200.012 (0.006)	1.79 (0.555)
	2.4	200.609 (0.304)	2.39 (0.416)	200.113 (0.056)	2.39 (0.416)
400	1.2	399.180 (0.205)	1.2 (0)	399.832 (0.042)	1.2 (0)
	1.8	395.488 (1.138)	1.8 (0)	400.037 (0.0092)	1.8 (0)
	2.4	397.737 (0.565)	2.4 (0)	400.213 (0.053)	2.39 (0.416)
600	1.2	600.001 (0.0001)	1.19 (0.84)	600.155 (0.025)	1.2 (0)
	1.8	600.960 (0.16)	1.8 (0)	600.143 (0.023)	1.8 (0)
	2.4	600.613 (0.102)	2.4 (0)	599.951 (0.0081)	2.39 (0.416)

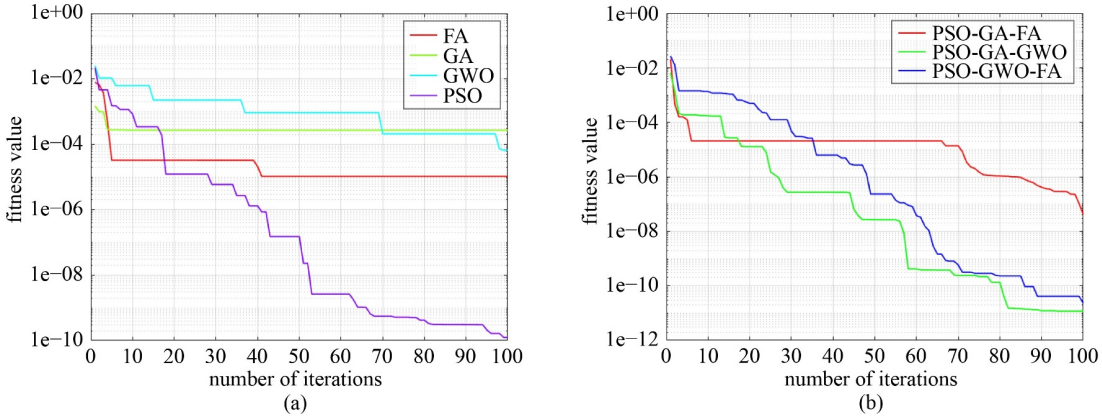

Fig. 5 Convergence of triple algorithms for case no. 6 for set A: (a) PSO, GA, FA, and GWO algorithms; (b) PSO-GA-FA, PSO-GA-GWO, and PSO-GWO-FA algorithms.

numerical results of the identification of the crack location and depth utilizing triple algorithms that are based on collections A to C are shown in Tables 9 and 10 for cases no. 2, 4, 8, and 10. Finally, Table 11 shows the best algorithm in each set for all cases.

Table 12 shows the standard deviation (SD) values of the best cost obtained after five independent performances of the PSO-GWO-FA algorithm and the computational time required for each run. It should be noted that all the results obtained and reported in Tables and Figures are based on assumptions of Table 4. Table 4 and the obtained results show that the proposed algorithms have better results when population and number of iterations are both larger. Also, population increase is an effective parameter in improving the performance of algorithms; increase in the number of iteration causes better convergency in the proposed algorithms.

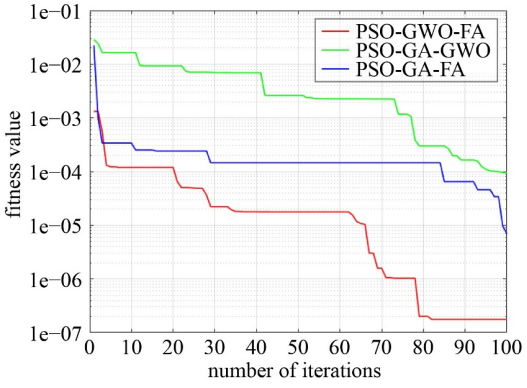

Fig. 6 Convergence of proposed triple algorithms for set A that have most errors for crack detection (PSO-GWO-FA: case no. 10, PSO-GA-GWO: case no. 8, PSO-GA-FA: case no. 7).

5 Conclusions

In this study, novel optimization algorithms are presented for crack detection in a cantilever Euler-Bernoulli beam. Methods using PSO-GWO-FA, PSO-GA-GWO, and PSO-GA-FA algorithms were created by modifying and improving PSO, GA, FA, and GWO algorithms to enhance their accuracy and speed of convergence. This paper explores variations between evaluated frequencies by the proposed algorithm and the measured frequencies for a cracked beam. The results of these proposed hybrid algorithms is compared with results of GA, GWO, FA, PSO, and MPSO. It is shown that the PSO-GA-FA algorithm in set A, the PSO-GWO-FA algorithm in set B, and the PSO-GWO-FA algorithm in set C have good

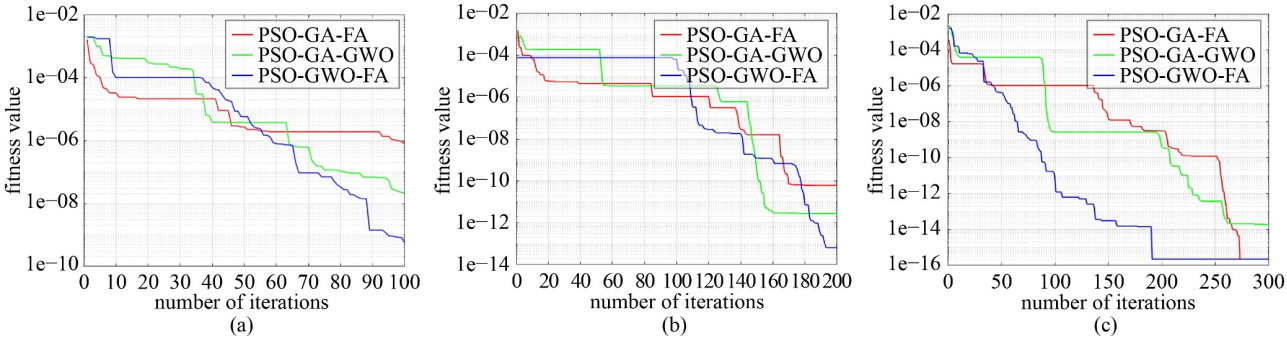

Fig. 7 Convergence of proposed triple hybrid algorithms for case no. 2: (a) set A, (b) set B and (c) set C.

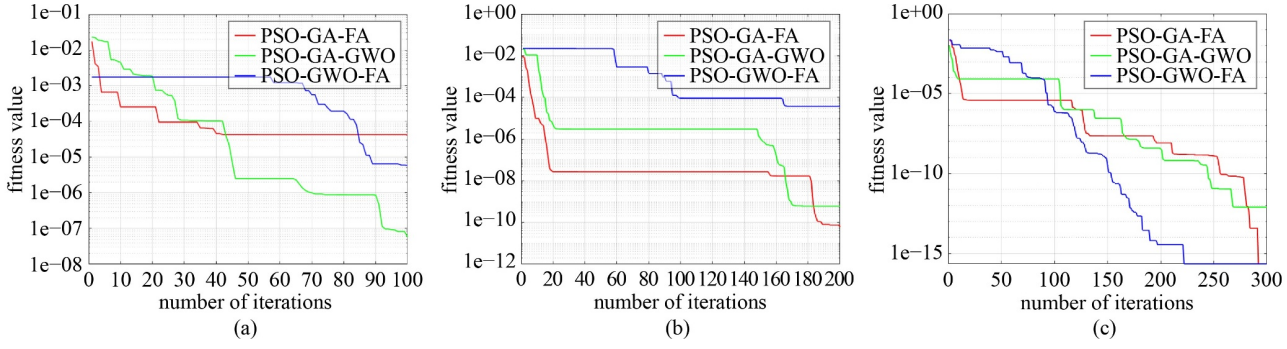

Fig. 8 Convergence of proposed triple hybrid algorithms for case no. 4: (a) set A, (b) set B and (c) set C.

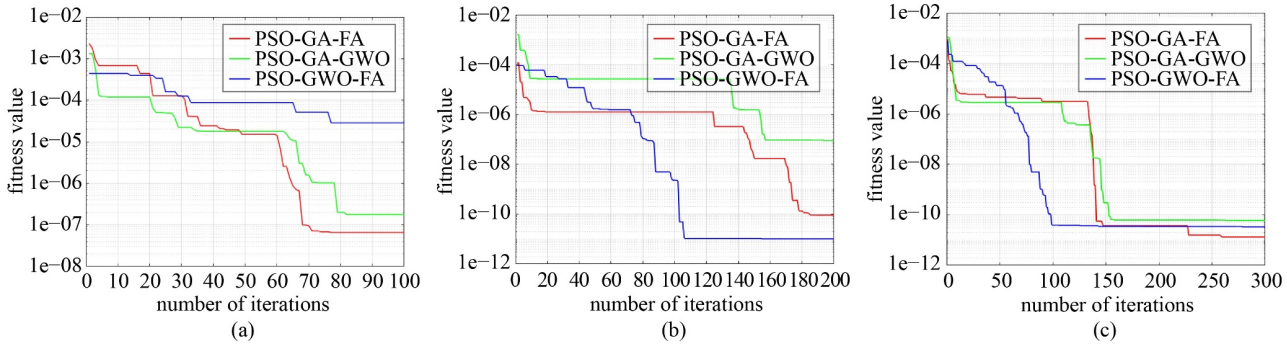

Fig. 9 Convergence of proposed triple hybrid algorithms for case no. 8: (a) set A, (b) set B and (c) set C.

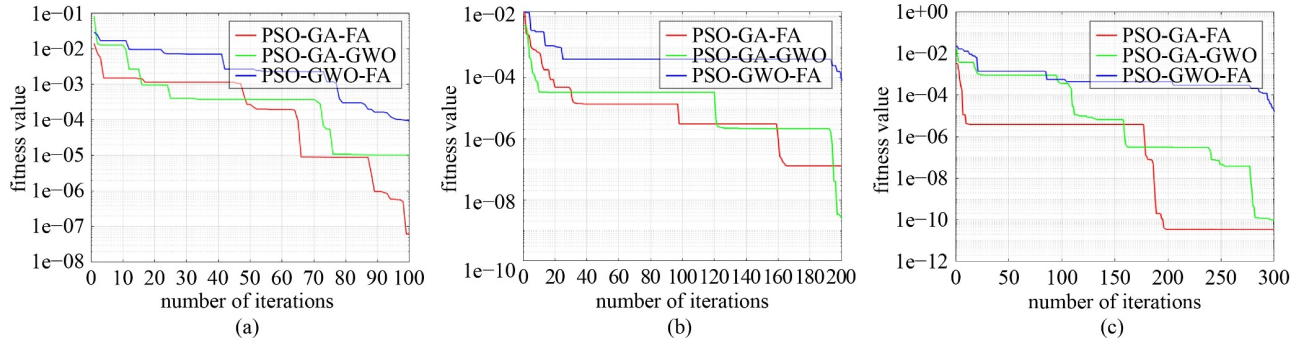

Fig. 10 Convergence of proposed triple hybrid algorithms for case no. 10: (a) set A, (b) set B and (c) set C.

Table 9 Numerical results of the crack detection by proposed triple algorithms for cases nos. 2 and 8

case no.	set	algorithm	predicted crack (mm)	
			Loc. (error%)	Dep. (error%)
case no. 2	set A	PSO-GWO-FA	200 (0)	1.2 (0)
		PSO-GA-GWO	199.999 (0.0005)	1.2 (0)
		PSO-GA-FA	200 (0)	1.19 (0.84)
	set B	PSO-GWO-FA	200 (0)	1.2 (0)
		PSO-GA-GWO	200 (0)	1.19 (0.84)
		PSO-GA-FA	200 (0)	1.19 (0.84)
	set C	PSO-GWO-FA	200 (0)	1.2 (0)
		PSO-GA-GWO	200 (0)	1.2 (0)
		PSO-GA-FA	200 (0)	1.2 (0)
case no. 8	set A	PSO-GWO-FA	599.908 (0.0153)	1.19 (0.84)
		PSO-GA-GWO	599.989 (0.0001)	1.19 (0.84)
		PSO-GA-FA	600 (0)	1.2 (0)
	set B	PSO-GWO-FA	600 (0)	1.2 (0)
		PSO-GA-GWO	599.999 (0.00016)	1.19 (0.84)
		PSO-GA-FA	599.997 (0.0005)	1.19 (0.84)
	set C	PSO-GWO-FA	600 (0)	1.2 (0)
		PSO-GA-GWO	599.999 (0.00016)	1.19 (0.84)
		PSO-GA-FA	599.999 (0.00016)	1.19 (0.84)

Table 10 Numerical results of the crack detection by proposed triple algorithms for cases nos. 4 and 10

case no.	set	algorithm	predicted crack (mm)	
			Loc. (error%)	Dep. (error%)
case no. 4	set A	PSO-GWO-FA	199.989 (0.005)	2.4 (0)
		PSO-GA-GWO	200 (0)	2.39 (0.416)
		PSO-GA-FA	200 (0)	2.39 (0.416)
	set B	PSO-GWO-FA	200 (0)	2.4 (0)
		PSO-GA-GWO	199.999 (0.0005)	2.4 (0)
		PSO-GA-FA	199.999 (0.0005)	2.4 (0)
	set C	PSO-GWO-FA	200 (0)	2.4 (0)
		PSO-GA-GWO	199.999 (0.0005)	2.4 (0)
		PSO-GA-FA	199.999 (0)	2.4 (0)
case no. 10	set A	PSO-GWO-FA	599.605 (0.065)	2.39 (0.416)
		PSO-GA-GWO	600.042 (0.007)	2.4 (0)
		PSO-GA-FA	599.999 (0.00016)	2.39 (0.416)
	set B	PSO-GWO-FA	600 (0)	2.4 (0)
		PSO-GA-GWO	600 (0)	2.4 (0)
		PSO-GA-FA	600 (0)	2.4 (0)
	set C	PSO-GWO-FA	600 (0)	2.4 (0)
		PSO-GA-GWO	599.999 (0.00016)	2.39 (0.416)
		PSO-GA-FA	599.999 (0.00016)	2.39 (0.416)

convergency for all cases. Therefore, it is concluded that the PSO-GA-FA and the PSO-GWO-FA algorithms have good accuracy in crack detection. The presented results show that the error in the crack detection using the proposed triple hybrid algorithms is approximately zero and the proposed algorithms provide improved accuracy relative to other algorithms, including those presented in previous studies in the identification of crack location and depth. These triple hybrid algorithms can be used for crack detection in structures under complex loadings.

Notations

PSO: Particle Swarm Optimization
GA: Genetic Algorithm
FA: Firefly Algorithm
GWO: Grey Wolf Optimization
EI: Flexural rigidity
PSO-GA-FA: Particle Swarm Optimization-Genetic Algorithm-Firefly Algorithm
PSO-GWO-FA: Particle Swarm Optimization-Grey

Wolf Optimization-Firefly Algorithm

PSO-GA-GWO: Particle Swarm Optimization-Genetic Algorithm-Grey Wolf Optimization

Table 11 Best algorithm to find crack detection

case no.	crack (mm)		best algorithm		
	Loc.	Dep.	set A	set B	set C
2	200	1.2	III	III	I-II-III
3	200	1.8	I-II	III	I-II-III
4	200	2.4	III	III	III
5	400	1.2	II-III	I-II	III
6	400	1.8	I-III	I-III	I-II-III
7	400	2.4	II	III	II
8	600	1.2	I	III	I-III
9	600	1.8	I	I	I
10	600	2.4	II	I-II-III	III

Note: I = PSO-GA-FA, II = PSO-GA-GWO, III = PSO-GWO-FA.

Table 12 SD of best cost and computational time of PSO-GWO-FA algorithm

case no.	set	time	Std
2	A	68.19	1.13e−08
	B	439.5	7.00e−09
	C	1439.22	2.40e−09
3	A	69.59	4.61e−0.8
	B`	419.29	4.28e−08
	C	1434.06	1.73e−08
4	A	61.62	1.22e−0.7
	B	381.37	4.52e−08
	C	1480.20	3.14e−14
5	A	54.99	6.60e−08
	B	394.55	2.09e−06
	C	1473.96	1.25e−13
6	A	59.22	4.31e−10
	B	438.62	9.93e−13
	C	1381.80	9.42e−15
7	A	61.71	9.71e−09
	B	430.29	5.86e−15
	C	1259.75	0
8	A	55.29	2.92e−09
	B	431.64	3.82e−12
	C	1322.15	3.92e−11
9	A	53.49	3.09e−08
	B	404.75	1.14e−10
	C	1364.90	1.99e−11
10	A	58.19	7.09e−07
	B	388.91	6.97e−08
	C	1321.61	2.13e−11

Appendix

B-Matrix is defined as:

$$\begin{vmatrix} 0 & 0 & 0 & 0 & 0 & 0 & 0 & 0 & 1 & 0 & 0 & 0 \\ 1 & 0 & 1 & 0 & 0 & 0 & 0 & 0 & 0 & 0 & 0 & 0 \\ 0 & 1 & 0 & 1 & 0 & 0 & 0 & 0 & 0 & 0 & 0 & 0 \\ 0 & 0 & 0 & 0 & 0 & 0 & 0 & 0 & 0 & 0 & -S_1 & S_2 \\ 0 & 0 & 0 & 0 & S_3 & S_4 & -S_5 & -S_6 & 0 & 0 & 0 & 0 \\ 0 & 0 & 0 & 0 & S_4 & S_3 & S_6 & -S_5 & 0 & 0 & 0 & 0 \\ 0 & 0 & 0 & 0 & 0 & 0 & 0 & 0 & S_7 & S_8 & -S_7 & -S_8 \\ S_9 & S_{10} & S_{11} & S_{12} & -S_9 & -S_{10} & -S_{11} & -S_{12} & 0 & 0 & 0 & 0 \\ S_9 & S_{10} & -S_{11} & -S_{12} & -S_9 & -S_{10} & S_{11} & S_{12} & 0 & 0 & 0 & 0 \\ S_{10} & S_9 & S_{12} & -S_{11} & -S_{10} & -S_9 & -S_{12} & S_{11} & 0 & 0 & 0 & 0 \\ S_{13} & S_{14} & S_{15} & S_{16} & S_{17} & S_{18} & S_{19} & S_{20} & S_{21} & S_{22} & S_{23} & S_{24} \\ S_{25} & S_{26} & S_{27} & S_{28} & S_{29} & S_{30} & S_{31} & S_{32} & S_{33} & S_{34} & S_{35} & S_{36} \end{vmatrix}$$

where

$S_1 = \sin H_s$, $S_2 = \cos H_s$, $S_3 = \cosh H_v$,
$S_4 = \sinh H_v$, $S_5 = \cos H_v$, $S_6 = \sin H_v$,
$S_7 = \cos (a \times H_s)$, $S_8 = \sin (a \times H_s)$, $S_9 = \cosh (a \times H_v)$,
$S_{10} = \sinh (a \times H_v)$, $S_{11} = \cos (a \times H_v)$, $S_{12} = \sin (a \times H_v)$,
$M_1 = H_v \times P_1$, $M_2 = H_s \times P_2$, $M_3 = H_v \times P_4$,
$M_4 = H_s \times P_1$, $M_5 = H_v \times P_3$, $S_{13} = M_1 \times S_{10}$,
$S_{14} = M_1 \times S_9$, $S_{15} = -M_1 \times S_{12}$, $S_{16} = M_1 \times S_{11}$,
$S_{17} = -M_1 \times S_{10}$, $S_{18} = -M_1 \times S_9$, $S_{19} = M_1 \times S_{12}$,
$S_{20} = -M_1 \times S_{11}$, $S_{21} = (-M_2 \times S_8 - M_2 \times P_1 \times S_8)$,
$S_{22} = (M_2 \times S_7 + M_4 \times P_2 \times S_7)$,
$S_{23} = M_2 \times S_8$, $S_{24} = -M_2 \times S_7$, $S_{25} = (M_3 \times S_{10} + M_5^2 \times P_4 \times S_9)$,
$S_{26} = (M_3 \times S_9 + M_3^2 \times P_3 \times S_{10})$, $S_{27} = (-M_3 \times S_{12} - M_5^2 \times P_4 \times S_{11})$, $S_{28} = (M_3 \times S_{11} - M_5^2 \times P_3 \times S_{12})$,
$S_{29} = -M_3 \times S_{10}$, $S_{30} = -M_3 \times S_9$, $S_{31} = M_3 \times S_{12}$,
$S_{32} = -M_3 \times S_{11}$, $S_{33} = P_3 \times S_7$, $S_{34} = P_3 \times S_8$,
$S_{35} = -P_3 \times S_7$, $S_{36} = -P_3 \times S_8$, $P_1 = \dfrac{AE}{LK_{11}}$,
$P_2 = \dfrac{AE}{K_{12}}$, $P_3 = \dfrac{EI}{LK_{22}}$, $P_4 = \dfrac{EI}{L^2 K_{21}}$.

References

1. Dimarogonas A, Papadopoulos C. Vibration of cracked shafts in bending. Journal of Sound and Vibration, 1983, 91(4): 583−593
2. Qian G L, Gu S N, Jiang J S. The dynamic behaviour and crack detection of a beam with a crack. Journal of Sound and Vibration, 1990, 138(2): 233−243
3. Nahvi H, Jabbari M. Crack detection in beams using experimental modal data and finite element model. International Journal of Mechanical Sciences, 2005, 47(10): 1477−1497
4. Chondros T, Dimarogonas A, Yao J. A continuous cracked beam vibration theory. Journal of Sound and Vibration, 1998, 215(1): 17−34
5. Kim J T, Stubbs N. Crack detection in beam-type structures using frequency data. Journal of Sound and Vibration, 2003, 259(1): 145−160

6. Orhan S. Analysis of free and forced vibration of a cracked cantilever beam. NDT & E International, 2007, 40(6): 443−450
7. Saavedra P, Cuitino L. Crack detection and vibration behavior of cracked beams. Computers & Structures, 2001, 79(16): 1451−1459
8. Zheng D Y, Kessissoglou N. Free vibration analysis of a cracked beam by finite element method. Journal of Sound and Vibration, 2004, 273(3): 457−475
9. Rizos P, Aspragathos N, Dimarogonas A. Identification of crack location and magnitude in a cantilever beam from the vibration modes. Journal of Sound and Vibration, 1990, 138(3): 381−388
10. Sahoo B, Maity D. Damage assessment of structures using hybrid neuro-genetic algorithm. Applied Soft Computing, 2007, 7(1): 89−104
11. Vakil Baghmisheh M T, Peimani M, Sadeghi M H, Ettefagh M M, Tabrizi A F. A hybrid particle swarm–Nelder–Mead optimization method for crack detection in cantilever beams. Applied Soft Computing, 2012, 12(8): 2217−2226
12. Vakil-Baghmisheh M T, Peimani M, Sadeghi M H, Ettefagh M M. Crack detection in beam-like structures using genetic algorithms. Applied Soft Computing, 2008, 8(2): 1150−1160
13. Patil D, Maiti S. Experimental verification of a method of detection of multiple cracks in beams based on frequency measurements. Journal of Sound and Vibration, 2005, 281(1−2): 439−451
14. Rosales M B, Filipich C P, Buezas F S. Crack detection in beam-like structures. Engineering Structures, 2009, 31(10): 2257−2264
15. Moezi S A, Zakeri E, Zare A, Nedaei M. On the application of modified cuckoo optimization algorithm to the crack detection problem of cantilever Euler–Bernoulli beam. Computers & Structures, 2015, 157: 42−50
16. Nandwana B, Maiti S. Detection of the location and size of a crack in stepped cantilever beams based on measurements of natural frequencies. Journal of Sound and Vibration, 1997, 203(3): 435−446
17. Lele S, Maiti S. Modelling of transverse vibration of short beams for crack detection and measurement of crack extension. Journal of Sound and Vibration, 2002, 257(3): 559−583
18. Viola E, Federici L, Nobile L. Detection of crack location using cracked beam element method for structural analysis. Theoretical and Applied Fracture Mechanics, 2001, 36(1): 23−35
19. Rezanezhad M, Lajevardi S A, Karimpouli S. An investigation on prevalent strategies for XFEM-based numerical modeling of crack growth in porous media. Frontiers of Structural and Civil Engineering, 2021, 15(4): 914−936
20. Rungamornrat J, Chansavang B, Phongtinnaboot W, Van C N. Investigation of Generalized SIFs of cracks in 3D piezoelectric media under various crack-face conditions. Frontiers of Structural and Civil Engineering, 2020, 14(2): 280−298
21. Zainud-Deen S H, Hassen W M, Awadalla K H. Crack detection using a hybrid finite difference frequency domain and particle swarm optimization techniques. In: 2009 National Radio Science Conference. Cairo: IEEE, 2009, 1−8
22. Nanthakumar S S, Lahmer T, Rabczuk T. Detection of flaws in piezoelectric structures using extended FEM. International Journal for Numerical Methods in Engineering, 2013, 96(6): 373−389
23. Nanthakumar S S, Lahmer T, Zhuang X, Zi G, Rabczuk T. Detection of material interfaces using a regularized level set method in piezoelectric structures. Inverse Problems in Science and Engineering, 2016, 24(1): 153−176
24. Nanthakumar S S, Lahmer T, Rabczuk T. Detection of multiple flaws in piezoelectric structures using XFEM and level sets. Computer Methods in Applied Mechanics and Engineering, 2014, 275: 98−112
25. Samanta S, Nanthakumar S S, Annabattula R K, Zhuang X. Detection of void and metallic inclusion in 2D piezoelectric cantilever beam using impedance measurements. Frontiers of Structural and Civil Engineering, 2019, 13(3): 542−556
26. Rabczuk T, Belytschko T. Cracking particles: A simplified meshfree method for arbitrary evolving cracks. International Journal for Numerical Methods in Engineering, 2004, 61(13): 2316−2343
27. Rabczuk T, Zi G, Bordas S, Nguyen-Xuan H. A geometrically non-linear three-dimensional cohesive crack method for reinforced concrete structures. Engineering Fracture Mechanics, 2008, 75(16): 4740−4758
28. Ghasemi H, Park H S, Rabczuk T. A level-set based IGA formulation for topology optimization of flexoelectric materials. Computer Methods in Applied Mechanics and Engineering, 2017, 313: 239−258
29. Ghasemi H, Park H S, Rabczuk T. A multi-material level set-based topology optimization of flexoelectric composites. Computer Methods in Applied Mechanics and Engineering, 2018, 332: 47−62
30. Ghasemi H, Kerfriden P, Bordas S P A, Muthu J, Zi G, Rabczuk T. Interfacial shear stress optimization in sandwich beams with polymeric core using non-uniform distribution of reinforcing ingredients. Composite Structures, 2015, 120: 221−230
31. Ghasemi H, Kerfriden P, Bordas S P A, Muthu J, Zi G, Rabczuk T. Probabilistic multiconstraints optimization of cooling channels in ceramic matrix composites. Composites. Part B, Engineering, 2015, 81: 107−119
32. Talebi H, Silani M, Rabczuk T. Concurrent multiscale modeling of three dimensional crack and dislocation propagation. Advances in Engineering Software, 2015, 80: 82−92
33. Zhou S, Rabczuk T, Zhuang X. Phase field modeling of quasi-static and dynamic crack propagation: COMSOL implementation and case studies. Advances in Engineering Software, 2018, 122: 31−49
34. Zhou S, Zhuang X, Zhu H, Rabczuk T. Phase field modelling of crack propagation, branching and coalescence in rocks. Theoretical and Applied Fracture Mechanics, 2018, 96: 174−192
35. Zhou S, Zhuang X, Rabczuk T. A phase-field modeling approach of fracture propagation in poroelastic media. Engineering Geology, 2018, 240: 189−203
36. Jena P K, Parhi D R. A modified particle swarm optimization technique for crack detection in Cantilever Beams. Arabian Journal for Science and Engineering, 2015, 40(11): 3263−3272
37. Ghannadiasl A, Ajirlou S K. Analytical solution of dynamic analysis of cracked Euler–Bernoulli beam with elastic boundary condition by GFM. Romanian Journal of Acoustics and Vibration, 2018, 15(2): 100−107
38. Ghadimi S, Kourehli S S. Crack detection of structures using modified extreme learning machine (MELM). Inverse Problems in

Science and Engineering, 2017, 25(7): 995−1013
39. Ghadimi S, Kourehli S S. Multiple crack identification in Euler beams using extreme learning machine. KSCE Journal of Civil Engineering, 2017, 21(1): 389−396
40. Prawin J, Rama Mohan Rao A. Reference-free breathing crack identification of beam-like structures using an enhanced spatial Fourier power spectrum with exponential weighting functions. International Journal of Structural Stability and Dynamics, 2019, 19(2): 1950017
41. Ghadimi S, Kourehli S S. Multi cracks detection in Euler-Bernoulli beam subjected to a moving mass based on acceleration responses. Inverse Problems in Science and Engineering, 2018, 26(12): 1728−1748
42. Samir K, Brahim B, Capozucca R, Abdel Wahab M. Damage detection in CFRP composite beams based on vibration analysis using proper orthogonal decomposition method with radial basis functions and cuckoo search algorithm. Composite Structures, 2018, 187: 344−353
43. Khatir S, Dekemele K, Loccufier M, Khatir T, Abdel Wahab M. Crack identification method in beam-like structures using changes in experimentally measured frequencies and Particle Swarm Optimization. Comptes Rendus Mécanique, 2018, 346(2): 110−120
44. Wimarshana B, Wu N, Wu C. Application of entropy in identification of breathing cracks in a beam structure: Simulations and experimental studies. Structural Health Monitoring, 2018, 17(3): 549−564
45. Wei Z, Liu J, Lu Z. Structural damage detection using improved particle swarm optimization. Inverse Problems in Science and Engineering, 2018, 26(6): 792−810
46. Khatir S, Abdel Wahab M, Boutchicha D, Khatir T. Structural health monitoring using modal strain energy damage indicator coupled with teaching-learning-based optimization algorithm and isogoemetric analysis. Journal of Sound and Vibration, 2019, 448: 230−246
47. Zenzen R, Belaidi I, Khatir S, Abdel Wahab M. A damage identification technique for beam-like and truss structures based on FRF and Bat Algorithm. Comptes Rendus Mécanique, 2018, 346(12): 1253−1266
48. Wang T, Noori M, Altabey W A. Identification of cracks in an Euler–Bernoulli beam using Bayesian inference and closed-form solution of vibration modes. Proceedings of the Institution of Mechanical Engineers, Part L: Journal of Materials: Design and Applications, 2021, 235(2): 421−438
49. Chinka S S B, Putti S R, Adavi B K. Modal testing and evaluation of cracks ofdn cantilever beam using mode shape curvatures and natural frequencies. Structures, 2021, 32(1): 1386−1397
50. Wu Z, Huang B, Tee K F, Zhang W. A novel stochastic approach for static damage identification of beam structures using homotopy analysis algorithm. Sensors (Basel), 2021, 21(7): 2366
51. Broumand P. Inverse problem techniques for multiple crack detection in 2D elastic continua based on extended finite element concepts. Inverse Problems in Science and Engineering, 2021, 29(12): 1702−1728
52. Casciati S. Stiffness identification and damage localization via differential evolution algorithms. Structural Control and Health Monitoring, 2008, 15(3): 436−449
53. Casciati S, Elia L. Potential of two metaheuristic optimization tools for damage localization in civil structures. Journal of Aerospace Engineering, 2017, 30(2): B4016012
54. Kennedy J, Eberhart R. Particle swarm optimization. In: Proceedings of ICNN'95—International Conference on Neural Networks. Perth: IEEE, 1995, 1942−1948
55. Yang X S. Firefly algorithm, stochastic test functions and design optimisation. International Journal of Bio-inspired Computation, 2010, 2(2): 78−84
56. Yang X S. Firefly algorithms for multimodal optimization. In: International Symposium on Stochastic Algorithms. Berlin: Spriner, 2009, 169−178
57. Mirjalili S, Mirjalili S M, Lewis A. Grey wolf optimizer. Advances in Engineering Software, 2014, 69: 46−61
58. Ghannadiasl A, Khodapanah Ajirlou S. Forced vibration of multi-span cracked Euler–Bernoulli beams using dynamic Green function formulation. Applied Acoustics, 2019, 148: 484−494